

# Supporting Information

## Bi-stability of contact angle and its role in achieving quantum-thin self-assisted GaAs nanowires

Wonjong Kim<sup>1†</sup>, Jelena Vukajlovic-Plestina<sup>1</sup>, Gözde Tütüncüoğlu<sup>1</sup>, Luca Francaviglia<sup>1</sup>, Lucas Güniat<sup>1</sup>, Heidi Potts<sup>1</sup>, Martin Friedl<sup>1</sup>, Jean-Baptiste Leran<sup>1</sup>,  
Anna Fontcuberta i Morral<sup>\*1</sup>

<sup>1</sup>Laboratory of Semiconductor Materials, Institute of Materials, École Polytechnique Fédérale de Lausanne, 1015 Lausanne, Switzerland

### SI 1 Contact angle analysis

Two stable contact angles are demonstrated with cross-section SEM and TEM images as shown in Fig.1. From NWs to NNs transition, we can also notice at the end of the tip having a stable radius of 10 nm.

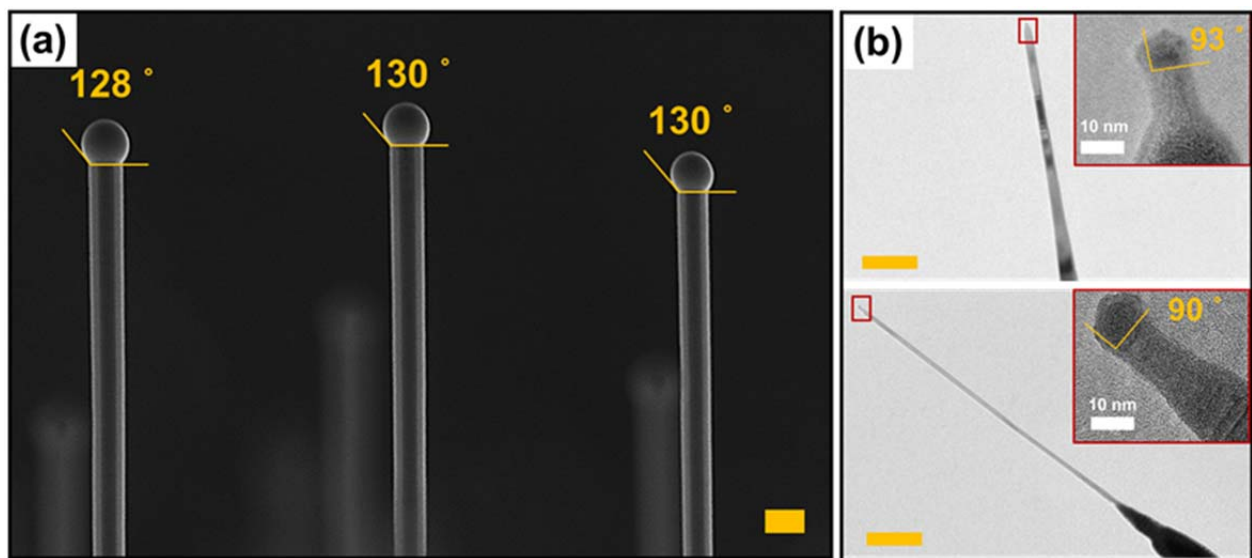


Figure 1. Ga droplet contact angle analysis. (a) cross-section SEM image of thick NWs and (b) thin NNs. The scale bars indicate 200 nm.

# Supporting Information

## SI 2 TEM analysis of other nanowires

Fig. 2 and 3 report two further examples of NWs with NNs. The TEM images confirm the trend reported in the manuscript: WZ becomes more frequent while moving from the NW stem to the NN. This is evident in the NW in fig. 1. Some NWs already show WZ at their bottom, like the one in fig. 2, in which case the NN is still mainly WZ.

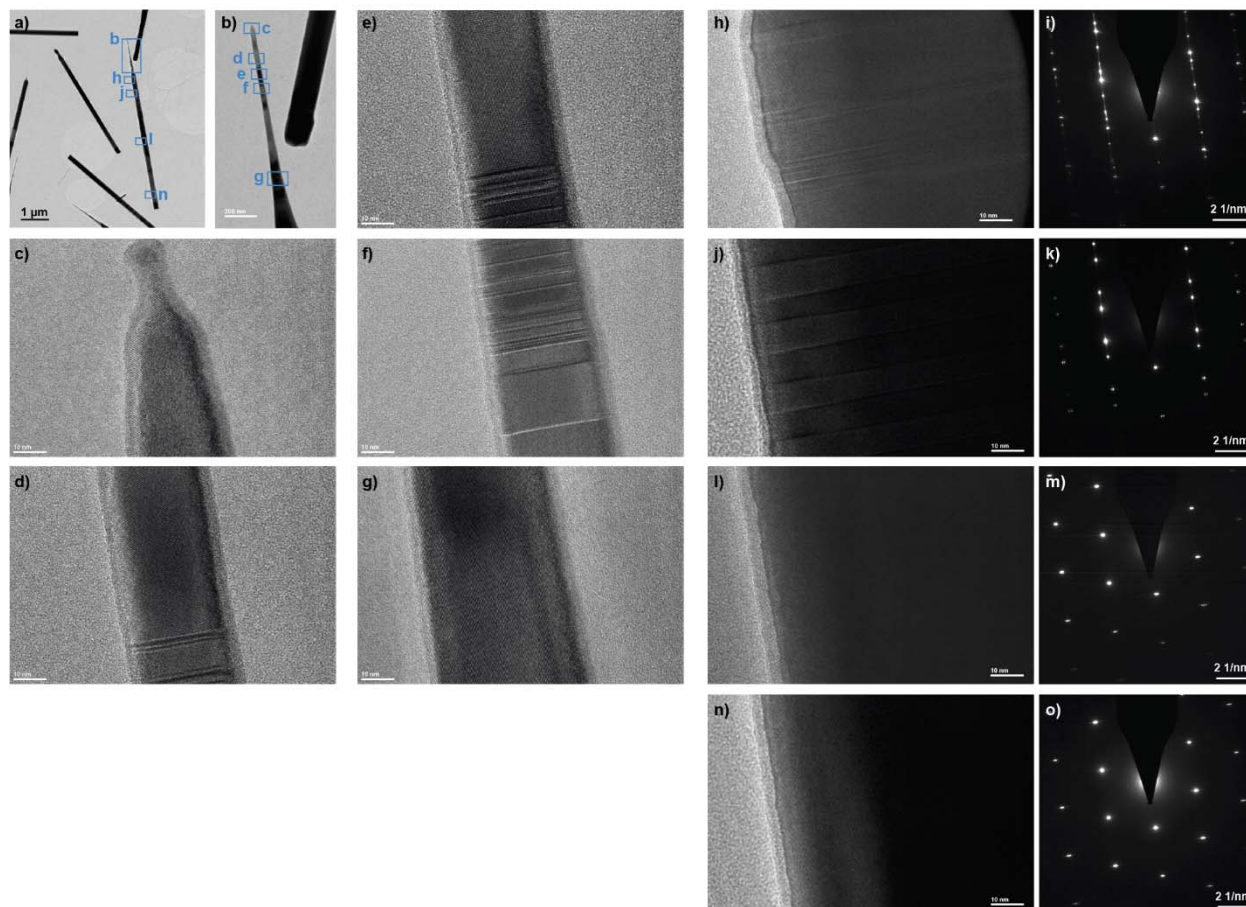


Figure 2. TEM images and diffraction patterns of a NW with NN. A-b) large overview of the NW. c-g) HRTEM images of the NN. Large WZ segments are present together with ZB. h-j-l-n) HRTEM images of the NW and related diffraction patterns i-k-m-o). The portion closer to the NN (h-i) shows a mixture of ZB and WZ. Farther down the NW stem (j-k) ZB twins alternate. The rest of the NW stem (l-o) is pure ZB.

# Supporting Information

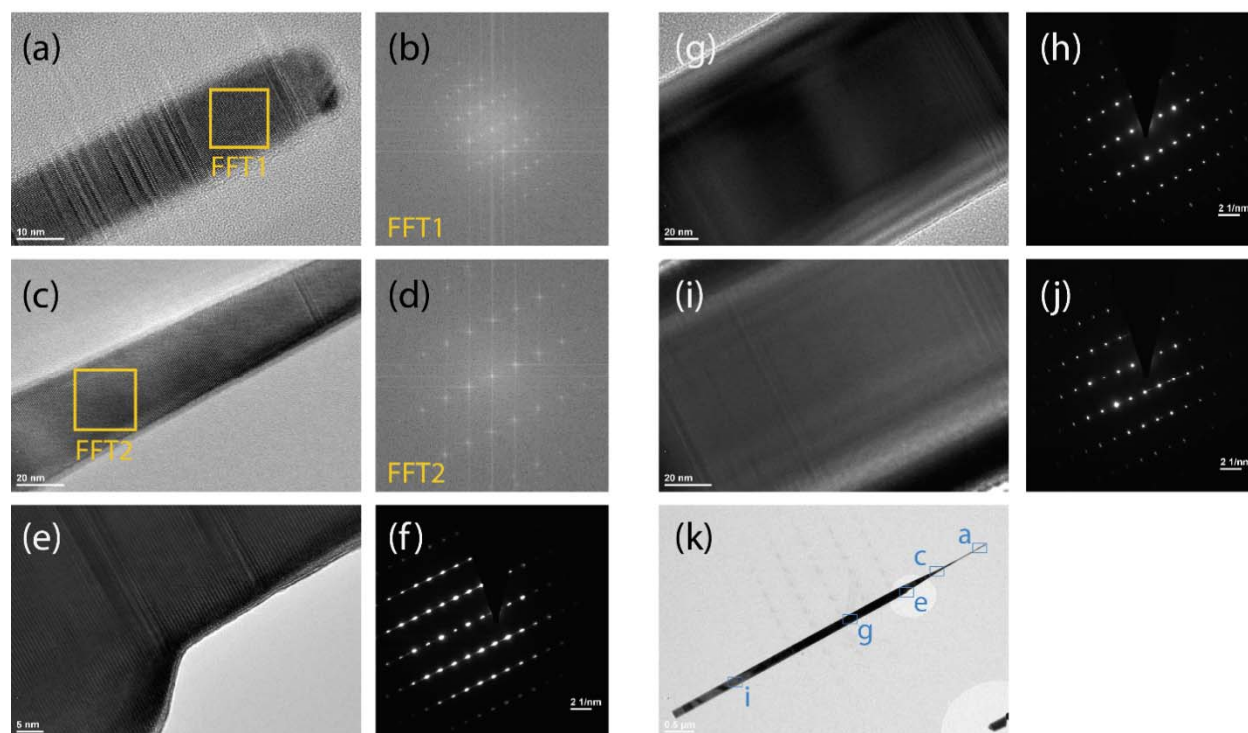


Figure 3 TEM images, diffraction patterns and FFT of a NW with NN. k) shows an overview of the NW. both the HR TEM images (a-c-e-g-i) and the corresponding FFT (b-d) or diffraction patterns (f-h-j) show that WZ is the predominant crystal phase along the full length of this NW.

## SI3 Nanowire radius evolution

From time series paper as mentioned in the manuscript Ref. [23], the droplet radius is almost linearly increased with time after an incubation time. The experimental values of the radius of nanowire stem are taken from SEM images as shown in Fig.4 and Fig. 5.

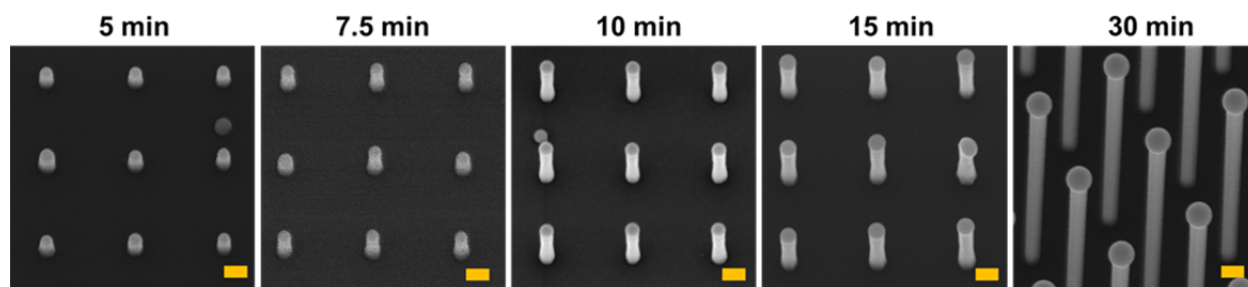


Figure 4. SEM images of the GaAs nanowire arrays demonstrating radius evolution with different growth time. The inter-wire spacing of 400 nm, the scale bars indicate 100 nm and the tilt angle of 20°.

# Supporting Information

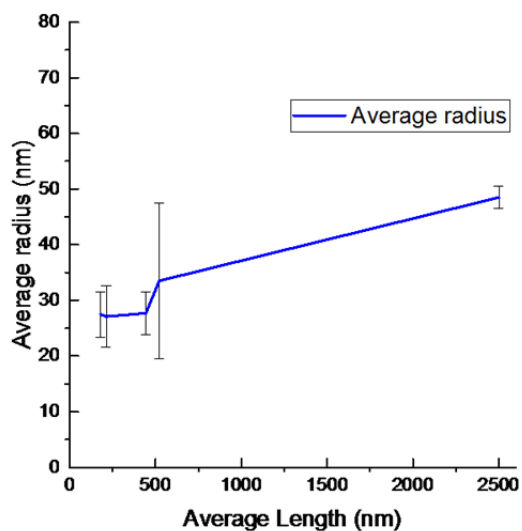


Figure 5. Average stem radius evolution of GaAs nanowires versus average length of GaAs nanowires. The data was obtained from the inter-wire spacing of 400 nm.

## Si4 Ga droplet at the end of the NNs

As shown in Figure 5, some wire still has droplet on the top of the NN and some doesn't.

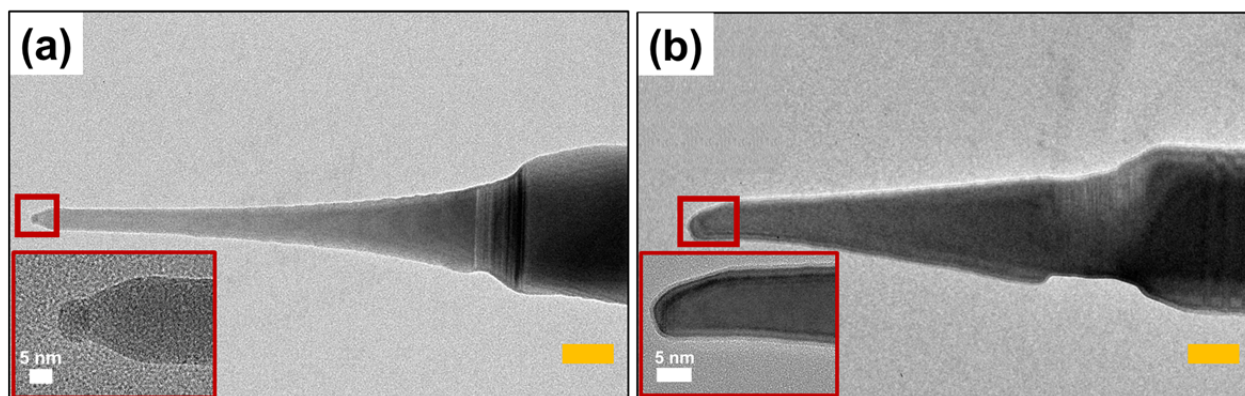
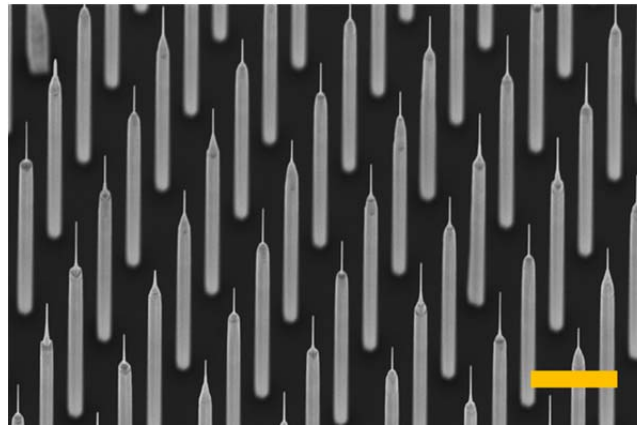


Figure 6. TEM images of top of the NNs show Ga droplet can be (a) still existed and (b) all consumed. The scale bars indicate 50 nm.

# Supporting Information

## SI5 Wider field characterization of nanoneedle fields



**Figure 7.** Regular arrays of the GaAs NN-on-NW structures with a spacing of 1000 nm, obtained via the three-step growth procedure. The scale bar indicates 1  $\mu\text{m}$ .

## SI6 Raman spectra

Figure 8 shows the Raman spectra collected from three NWs under the same measurement conditions (see methods in the manuscript). For each NW, we compare the Raman signal collected at the NN and at the NW base.

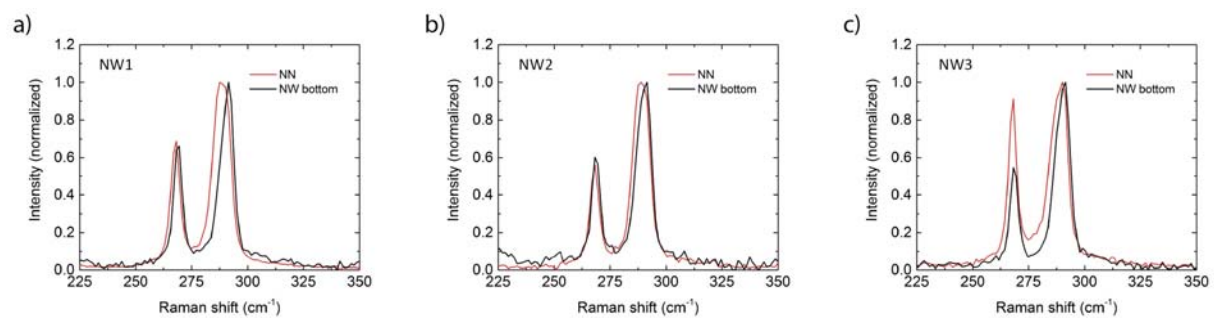


**Figure 8.** Raman spectra of three different NWs collected at the NW bottoms (black) and at the NN (red). The spectra are normalized with respect to the LO peak in order to ease up the observation of the peak broadening and downshift.